5460 *Inorg. Chem.* **2010**, *49*, 5460–5471
DOI: 10.1021/ic1000123

Inorganic Chemistry
Article

# $Cr^{III}-Cr^{III}$ Interactions in Two Alkoxo-Bridged Heterometallic $Zn_2Cr_2$ Complexes Self-Assembled from Zinc Oxide, Reinecke's Salt, and Diethanolamine

**Valentyna V. Semenaka,[†] Oksana V. Nesterova,[†] Volodymyr N. Kokozay,[†] Viktoriya V. Dyakonenko,[‡] Roman I. Zubatyuk,[‡] Oleg V. Shishkin,[‡,§] Roman Boča,[⊥] Julia Jezierska,[¶] and Andrew Ozarowski*[,□]**

[†]*Department of Inorganic Chemistry, National Taras Shevchenko University, Volodymyrska Street 64, Kyiv 01601, Ukraine,* [‡]*STC "Institute for Single Crystals", National Academy of Sciences of Ukraine, 60 Lenin Avenue, Kharkiv 61001, Ukraine,* [§]*Department of Inorganic Chemistry, V. N. Karazin Kharkiv National University, 4 Svobody Sq., Kharkiv 61077, Ukraine,* [⊥]*Institute of Inorganic Chemistry, FCHPT, Slovak University of Technology, Radlinskeho 9, 81237 Bratislava, Slovakia,* [¶]*Faculty of Chemistry, University of Wroclaw, F. Joliot-Curie Street 14, 50-383 Wroclaw, Poland, and* [□]*National High Magnetic Field Laboratory, Florida State University, 1800 East Paul Dirac Drive, Tallahassee, Florida 32310*

Received January 4, 2010

Two new tetranuclear complexes, $[Zn_2Cr_2(NCS)_4(Dea)_2(HDea)_2]\cdot 4DMSO$ (**1**; DMSO = dimethyl sulfoxide) and $[Zn_2Cr_2(NCS)_4(Dea)_2(HDea)_2]\cdot 2CH_3CN$ (**2**), were prepared from zinc oxide, Reinecke's salt, $NH_4[Cr(NCS)_4(NH_3)_2]\cdot H_2O$, ammonium thiocyanate, and a nonaqueous solution of diethanolamine ($H_2Dea$) in a reaction carried out under open air. Both compounds have similar centrosymmetric crystal structures based on a tetranuclear $\{Zn_2Cr_2(\mu_3\text{-}O)_2(\mu\text{-}O)_4\}$ core. Variable-temperature magnetic susceptibility measurements of **1** and **2** show weak antiferromagnetic coupling between chromium centers. The magnetic data and high-field, high-frequency electron paramagnetic resonance spectra were analyzed in terms of the spin Hamiltonian

$$\hat{H} = J\hat{\boldsymbol{S}}_1\cdot\hat{\boldsymbol{S}}_2 - j(\hat{\boldsymbol{S}}_1\cdot\hat{\boldsymbol{S}}_2)^2 + \mu_B\boldsymbol{B}\{g_1\}\hat{\boldsymbol{S}}_1 + D_{Cr}\{\hat{\boldsymbol{S}}_{z1}^2 - S_1(S_1+1)/3\} + E_{Cr}(\hat{\boldsymbol{S}}_{x1}^2 - \hat{\boldsymbol{S}}_{y1}^2) + \mu_B\boldsymbol{B}\{g_2\}\hat{\boldsymbol{S}}_2 + D_{Cr}\{\hat{\boldsymbol{S}}_{z2}^2 - S_2(S_2+1)/3\} + E_{Cr}(\hat{\boldsymbol{S}}_{x2}^2 - \hat{\boldsymbol{S}}_{y2}^2) + D_{12}\{\hat{\boldsymbol{S}}_{z1}\hat{\boldsymbol{S}}_{z2} - \hat{\boldsymbol{S}}_1\cdot\hat{\boldsymbol{S}}_2/3\} + E_{12}(\hat{\boldsymbol{S}}_{x1}\hat{\boldsymbol{S}}_{x2} - \hat{\boldsymbol{S}}_{y1}\hat{\boldsymbol{S}}_{y2})$$

with $J = 13.7\ cm^{-1}$, $j = 1.1\ cm^{-1}$, $D_{Cr} = 0.3864\ cm^{-1}$, $E_{Cr} = -0.1104\ cm^{-1}$, $D_{12} = -0.1873\ cm^{-1}$, and $E_{12} = -0.0155\ cm^{-1}$ for **1** and $J = 9.4\ cm^{-1}$, $j = 0.8\ cm^{-1}$, $D_{Cr} = 0.3564\ cm^{-1}$, $E_{Cr} = -0.0647\ cm^{-1}$, $D_{12} = -0.1850\ cm^{-1}$, and $E_{12} = -0.0112\ cm^{-1}$ for **2**. Density functional theory (DFT) calculations were employed to calculate the zero-field splitting on $Cr^{3+}$ ions. Calculations of the exchange integrals $J$ were attempted by using the "broken-symmetry" DFT method.

## Introduction

In the last few decades, the investigation of the structures and properties of heterometallic complexes of paramagnetic metals has become the focus of extensive research because of their potential advanced application, including catalysis, biological systems modeling, and molecular magnetism.[1] Also, since the discovery of the first single-molecule magnet in 1993,[2] the synthesis and physical characterization of polynuclear clusters of paramagnetic metal ions have become some of the most active fields in coordination chemistry.[3] Increased interest in the magnetic properties of chromium-containing compounds dates from the late 1990s, largely because of Winpenny's investigations on polynuclear chromium cages and wheels.[3b] However, the rational synthesis of heterometallic chromium clusters still remains a challenge. The formation of oxo-bridged polynuclear complexes of paramagnetic transition- and rare-earth-metal ions, derived from polyalcoholato ligands is poorly understood.[4] Our systematic studies have demonstrated that amino alcohols

*To whom correspondence should be addressed. E-mail: ozarowsk@magnet.fsu.edu. Tel.:850-644-5996. Fax: 850-644-1366.

(1) (a) Müller, A.; Peters F.; Pope, M. T.; Gatteschi, D. *Chem. Rev.* **1998**, *98*, 239−271 and references cited therein. (b) Pope, M. T.; Müller, A. *Angew. Chem., Int. Ed. Engl.* **1991**, *30*, 34–48. (c) Taft, K. L.; Delfs, C. D.; Papaefthymiou, G. C.; Foner, S.; Gatteschi, D.; Lippard, S. *J. Am. Chem. Soc.* **1994**, *116*, 823–832.

(2) Sessoli, R.; Gatteschi, D.; Caneschi, A.; Novak, M. A. *Nature* **1993**, *365*, 141–142.

(3) For example, see:(a) Sessoli, R.; Gatteschi, D. *Angew. Chem., Int. Ed.* **2003**, *42*, 268–297. (b) McInnes, E. J. L.; Piligkos, S.; Timco, G. A.; Winpenny, R. E. P. *Coord. Chem. Rev.* **2005**, *249*, 2577–2590. (c) Affronte, M.; Casson, I.; Evangelisti, M.; Candini, A.; Carretta, S.; Muryn, C. A.; Teat, S. J.; Timco, G. A.; Wernsdorfer, W.; Winpenny, R. E. P. *Angew. Chem., Int. Ed.* **2005**, *44*, 6496–6500.

 Published on Web 05/24/2010 

represent a powerful tool for assembling polynuclear metal complexes in "one-pot" reactions using zerovalent metals along with metal salts as starting materials.[5] This direct synthesis of coordination compound strategy yielded numerous heterobimetallic ($M^1/M^2$; $M^1$ = Cu; $M^2$ = Zn, Pb, Cd, Co; X = halide, NCS, OAc; HL = amino alcohols) complexes.[6] Now, we are extending our studies to M/Cr (M = Cu, Co, Zn) systems. Recently, we have shown that Reinecke's salt, $NH_4[Cr(NCS)_4(NH_3)_2]\cdot H_2O$, could be used as a source of building blocks for the synthesis of polymeric and ionic Cu/Cr heterometallic compounds based on amines (L) and open-chain Schiff-based ligands.[7] At the same time, it appeared that Reinecke's salt under direct synthesis conditions can disintegrate and supply Cr to form more complicated structures of higher nuclearity.[8] With the aim to obtain heteropolynuclear species, the system $ZnO-NH_4[Cr(NCS)_4(NH_3)_2]-H_2Dea-NH_4NCS-Solv$ was chosen ($H_2Dea$ = diethanolamine). Herein, we report the synthesis, crystal structure, and spectroscopic and magnetic investigations of the two new tetranuclear clusters $[Zn_2Cr_2(NCS)_4(Dea)_2(HDea)_2]\cdot 4DMSO$ (**1**; DMSO = dimethyl sulfoxide) and $[Zn_2Cr_2(NCS)_4(Dea)_2(HDea)_2]\cdot 2CH_3CN$ (**2**) prepared from zinc oxide by the decomposition of Reinecke's salt in the presence of diethanolamine. Diethanolamine was chosen as a ligand because of its bifunctional nature, which enables it to serve in a variety of coordination modes. The chemistry of diethanolamine derivatives has been thoroughly investigated only with iron,[9] manganese,[10] and nickel.[11] The Cambridge database (version 5.30, Nov 2008) reveals that there are only a handful of zinc complexes containing amino alcohols as bridging ligands, including only one chromium complex. These include star-shaped heteronuclear $[Cr\{Fe(L)_2\}_3]$ cluster-containing methyl-substituted diethanolamine.[9a]

## Experimental Section

**Synthesis.** Zinc oxide (0.10 g, 1.25 mmol), $NH_4[Cr(NCS)_4(NH_3)_2]\cdot H_2O$ (0.89 g, 2.50 mmol), $NH_4NCS$ (0.09 g, 1.25 mmol), DMSO (15 $cm^3$), and diethanolamine (1 $cm^3$) were heated to 50−60 °C and stirred until complete dissolution of the zinc oxide was observed (ca. 180 min). Dark-violet crystals suitable for the X-ray crystallographic study were deposited from the resulting blue solution within several days after the successive addition of $Pr^iOH$. The crystals were filtered off, washed with dry $Pr^iOH$, and finally dried in vacuo at room temperature. Yield: 0.25 g, 17.2% (per zinc). Anal. Calcd for $C_{28}H_{62}Zn_2Cr_2N_8O_{12}S_8$ ($M$ = 1194.1): Zn, 10.95; Cr, 8.71; C, 28.16; H, 5.19; N, 9.38; S, 21.47. Found: Zn, 10.1; Cr, 8.8; C, 28.4; H, 5.1; N, 9.5; S, 21.0. IR: 3400(br), 3220(m), 3201(sh), 3123(m), 2974(sh), 2919(m), 2878(m), 2091(sh), 2080(vs), 2063(sh), 1635(s), 1491(sh), 1472(sh), 1452(sh), 1438(m), 1427(sh), 1398(w), 1378(w), 1351(sh), 1315(w), 1293(w), 1275(sh), 1237(w), 1156(w), 1110(sh), 1090(sh), 1032(s), 949(w), 916(w), 887(w), 878(sh), 823(sh), 635(m), 621(sh), 514(w), 460(w), 424(sh).

The synthesis of **2** was carried out analogously, using $CH_3CN$ instead of DMSO. Yield: 0.12 g, 10.25% (per zinc). Anal. Calcd for $C_{24}H_{44}Zn_2Cr_2N_{10}O_8S_4$ ($M$ = 963.75): Zn, 13.57; Cr, 10.79; C, 29.91; H, 4.56; N, 14.53; S, 26.61. Found: Zn, 13.5; Cr, 10.9; C, 28.5; H, 4.6; N, 14.5; S, 26.7. IR: 3164(w), 3156(sh), 3124(sh), 3117(m), 3111(sh), 3092(w), 3061(sh), 3047(sh), 3028(sh), 3003(m), 2896(m), 2403(w), 2090(vs), 1687(w), 1490(m), 1468(sh), 1345(sh), 1284(m), 1252(w), 1215(sh), 1167(w), 1143(sh), 1105(m), 1085(sh), 1057(sh), 996(w), 865(m), 815(w), 773(m), 708(m), 667(sh), 635(m), 610(sh), 585(m), 514(m), 477(m), 450(w), 426(w), 411(w).

**Magnetic Properties.** Magnetic susceptibility data of powdered samples were measured with a SQUID magnetometer (Quantum Design MPMSXL-5) over the temperature range 1.8−300 K at a magnetic induction of 0.5 T. Corrections for the sample holders were applied. Diamagnetic corrections for the molecules were determined from Pascal's constants.[12]

**Electron Paramagnetic Resonance (EPR) Spectra.** High-field, high-frequency EPR spectra at temperatures ranging from ca. 3 to 290 K were recorded on a home-built spectrometer at the EMR facility of NHMFL.[13] The instrument was a transmission-type device in which microwaves were propagated in cylindrical lightpipes. The microwaves were generated by a phase-locked Virginia Diodes source, generating a frequency of 13 ± 1 GHz and producing its harmonics, of which the 2nd, 4th, 6th, 8th, 16th, 24th, and 32nd were available. A superconducting magnet (Oxford Instruments) capable of reaching a field of 17 T was employed. X-band spectra (9.6 GHz) were recorded on a Bruker ESP-300 instrument at room temperature and at 77 K for powder samples and frozen dimethylformamide (DMF) solutions. X-band powder spectra of **1** at 40 K were taken on a Bruker ElexSys 680 instrument.

**X-ray Structure Determination.** Details of the data collection and processing, structure solution, and refinement are summarized in Table 1. X-ray diffraction data for **1** and **2** were collected on an XCalibur 3 diffractometer equipped with graphite-monochromated Mo Kα radiation ($\lambda$ = 0.710 73 Å). The structures

(4) (a) Winpenny, R. E. P. In *Perspectives in Supramolecular Chemistry*; Sauvage, J. P, Ed.; Wiley-VCH: Weinheim, Germany, 1999; Vol. *5*, pp193−223. (b) Pecoraro, V. L.; Stemmler, A. J.; Gibney, B. R.; Bodwin, J. J.; Wang, H.; Kampf., J.; Barwinsky, A. *Prog. Inorg. Chem.* **1997**, *45*, 83–177. (c) Cutland, A. D.; Malkani, R. G.; Kampf, J. W.; Pecoraro, V. L. *Angew. Chem., Int. Ed.* **2000**, *39*, 2689–2691. (d) Lah, M. S.; Pecoraro, V. L. *J. Am. Chem. Soc.* **1989**, *11*, 7258–7259. (e) Kessler, V. G. *Chem. Commun.* **2003**, 1213–1222.

(5) Kokozay, V. N.; Vassilyeva, O. Yu. *Transition Met. Chem.* **2002**, *27*, 693–699.

(6) (a) Kovbasyuk, L. A.; Vassilyeva, O. Yu.; Kokozay, V. N.; Linert, W.; Skelton, B. W.; Oliver, A. G. *New J. Chem.* **1998**, *22*, 931–932. (b) Makhankova, V. G.; Vassilyeva, O. Yu.; Kokozay, V. N.; Skelton, B. W.; Reedijk, J.; Van Albada, G. A.; Sorace, L.; Gatteschi, D. *New J. Chem.* **2001**, *25*, 685–689. (c) Nesterov, D. S.; Makhankova, V. G.; Vassilyeva, O. Yu.; Kokozay, V. N.; Kovbasyuk, L. A.; Skelton, B. W.; Jezierska, J. *Inorg. Chem.* **2004**, *43*, 7868–7876. (d) Nesterov, D. S.; Kokozay, V. N.; Skelton, B. W.; Jezierska, J. *Dalton Trans.* **2007**, 558–564.

(7) (a) Nikitina, V. M.; Nesterova, O. V.; Kokozay, V. N.; Goreshnic, E. A.; Jezierska, J. *Polyhedron* **2008**, *27*, 2426–2430. (b) Nikitina, V. M.; Nesterova, O. V.; Kokozay, V. N.; Dyakonenko, V. V.; Shishkin, O. V.; Jezierska, J. *Inorg. Chem. Commun.* **2009**, *12*, 101–104.

(8) (a) Semenaka, V. V.; Nesterova, O. V.; Kokozay, V. N.; Dyakonenko, V. V.; Shishkin, O. V.; Boca, R.; Jezierska, J. *Dalton Trans.* **2010**, *39*, 1734–1739. (b) Semenaka, V. V.; Nesterova, O. V.; Kokozay, V. N.; Zubatyuk, R.; Shishkin, O. V.; Boca, R.; Shevchenko, D. V.; Huang, P.; Styring, S. *Dalton Trans.* **2010**, *39*, 2344–2349.

(9) (a) Saalfrank, R. W.; Bernt, I.; Chowdhry, M. M.; Hampel, F.; Vaughan, G. B. M. *Chem.—Eur. J.* **2001**, *7*, 2765–2769. (b) Saalfrank, R. W.; Bernt, I.; Uller, E.; Hampel, F. *Angew. Chem., Int. Ed. Engl.* **1997**, *36*, 2482–2485. (c) Saalfrank, R. W.; Deutscher, C.; Sperner, S.; Nakajima, T.; Ako, A. M.; Uller, E.; Hampel, F.; Heinemann, F. W. *Inorg. Chem.* **2004**, *43*, 4372–4382. (d) Alco, A. M.; Mereacre, V.; Mereacre, I. J.; Hewitt, I. J.; Clèrac, R.; Lecren, L.; Anson, C. E.; Powell, A. K. *Mater. J. Chem.* **2006**, *16*, 2579–2586. (e) Alco, A. M.; Waldmann, O.; Mereacre, V.; Klöwer, F.; Hewitt, I. J.; Anson, C. E.; Güdel, H. U.; Powell, A. K. *Inorg. Chem.* **2007**, *46*, 756–766.

(10) (a) Foguet-Albiol, D.; O'Brien, T. A.; Wernsdorfer, W.; Moulton, B.; Zaworotko, M. J.; Abboud, K. A.; Christou, G. *Angew. Chem., Int. Ed.* **2005**, *44*, 897–901. (b) Murugesu, M.; Wernsdorfer, W.; Abboud, K. A.; Christou, G. *Angew. Chem., Int. Ed.* **2005**, *44*, 892–896. (c) Langley, S. K.; Berry, K. J.; Moubarakia, B.; Murray, K. S. *Dalton Trans.* **2009**, 973–982.

(11) (a) Saalfrank, R. W.; Bernt, I.; Hampel, F. *Chem.—Eur. J.* **2001**, *7*, 2770–2774. (b) Yilmaz, V. T.; Karadag, A.; ThËone, C.; Herbst-Irmer, R. *Acta. Crystallogr.* **2000**, *C56*, 948–949. (c) Foguet-Albiol, D.; Abboud, K. A.; Christou, G. *Chem. Commun.* **2005**, 4282–4284. (d) Ferguson, A.; Lawrence, J.; Parkin, A.; Sanchez-Benitez, J.; Kamenev, K. V.; Brechin, E. K.; Wernsdorfer, W.; Hill, S.; Murrie, M. *Dalton Trans.* **2008**, 6409–6414.

(12) O'Connor, C. J. *Prog. Inorg. Chem.* **1982**, *29*, 203–283.

(13) Hassan, A. K.; Pardi, L. A.; Krzystek, J.; Sienkiewicz, A.; Goy, P.; Rohrer, M.; Brunel, L.-C. *J. Magn. Reson.* **2000**, *142*, 300–312.

**Table 1.** Crystallographic and Refinement Data for **1** and **2**

| | | |
|---|---|---|
| empirical formula | $C_{20}H_{38}Cr_2N_8O_8S_4Zn_2 \cdot 4C_2H_6OS$ (**1**) | $C_{20}H_{38}Cr_2N_8O_8S_4Zn_2 \cdot 2CH_3CN$ (**2**) |
| fw | 1194.08 | 963.75 |
| $T$ [K] | 100(2) | 293(2) |
| cryst syst | triclinic | monoclinic |
| space group | $P\bar{1}$ | $P2(1)/n$ |
| $a$ [Å] | 9.782(5) | 9.824(2) |
| $b$ [Å] | 11.095(4) | 18.197(4) |
| $c$ [Å] | 12.188(5) | 11.807(3) |
| α [deg] | 93.36(3) | 90 |
| $\beta$ [deg] | 94.28(4) | 107.35(3) |
| $\gamma$ [deg] | 108.77(4) | 90 |
| $V$ [Å$^3$] | 1244.2(10) | 2014.71(8) |
| $Z$ | 1 | 1 |
| $\mu$ [mm$^{-1}$] | 1.772 | 1.962 |
| $F$(000) | 618 | 988 |
| measd reflns | 12 557 | 19 793 |
| obsd [$F > 4\sigma(F)$] | 4948 | 3433 |
| $R_{int}$ | 0.0246 | 0.0347 |
| $R$ [$F > 4\sigma(F)$] | 0.0320 | 0.0350 |
| wR (all data) | 0.0683 | 0.0862 |

were solved by direct methods and refined against $F^2$ by full-matrix least-squares methods using the *SHELXTL* package.[14] All non-H atoms were refined within anisotropic approximation. The H atoms were located from the difference map of the electron density and refined by a "riding" model with $U_{iso} = nU_{eq}$ of a carrier non-H atom ($n$ = 1.5 for methyl and 1.2 for other H atoms).

## Results and Discussion

The open-air reaction of zinc oxide, Reinecke's salt, and ammonium thiocyanate with diethanolamine dissolved in DMSO (**1**) or in $CH_3CN$ (**2**), using molar ratios ZnO:$NH_4$-$[Cr(NCS)_4(NH_3)_2]$:$NH_4NCS$ = 1:2:1, yielded dark-violet microcrystals that showed a 1:1 ratio of $Zn^{II}$ to $Cr^{III}$ (see the Synthesis section). The reaction appears to proceed in the following way:

$$2ZnO + 2NH_4[Cr(NCS)_4(NH_3)_2] + 9H_2Dea + NH_4NCS + m\text{Solv} \rightarrow [Zn_2Cr_2(NCS)_4(HDea)_2(Dea)_2] \cdot m\text{Solv} + 7NH_3 + 5H_2Dea \cdot HSCN + 2H_2O$$

The IR spectra of complexes **1** and **2** in the range of 4000−400 cm$^{-1}$ are quite similar and show all expected ligand peaks. The presence of hydrogen-bonded OH groups in **1** can be clearly observed in the spectra (bands at 3400 cm$^{-1}$), whereas free (≈3600 cm$^{-1}$) OH groups were not observed.[15] Bands corresponding to $\nu$(SO) vibrations of DMSO were clearly observed at 1032 cm$^{-1}$ in the spectra of **1**. The very strong bands at 2080(1) and 2090(2) cm$^{-1}$ and weak bands at 823(1) and 815(2) cm$^{-1}$ were attributed to the $\nu$(CN) and $\nu$(CS) vibrations, respectively. The frequencies of the observed bands imply coordination of the NCS group through the N atom,[14] in agreement with the crystal structures of our complexes.

**Structure Description.** X-ray diffraction studies reveal that the molecular structures of **1** and **2** (Figure 1 and Table 2) are based on a centrosymmetric $\{Zn_2Cr_2(\mu\text{-}O)_6\}$ core that belongs to the widespread $Ti_4(OMe)_{16}$ structural type.[16] All four metal atoms lie in one plane. Each Zn center displays tetrahedral coordination geometry, with two O atoms from the HDea and Dea ligands. The Zn−O(N) distances vary from 1.954(2) to 1.968(2) Å and the bond angles O(N)−Zn−O(N) from 104.83(7)° to 116.76(9)°. Both Cr atoms have a distorted octahedral geometry with the Cr−O(N) distances in the range 1.945(2)−2.095(2) Å, while the cis bond angles about Cr range from 81.00(7)° to 102.06(7)° and the trans bond angles from 160.79(6)° to 177.10(6)°. The $Cr_2O_2$ fragment is planar. The Dea and HDea ligands adopt a chelating−bridging mode, forming five-membered rings. Both O atoms of the Dea

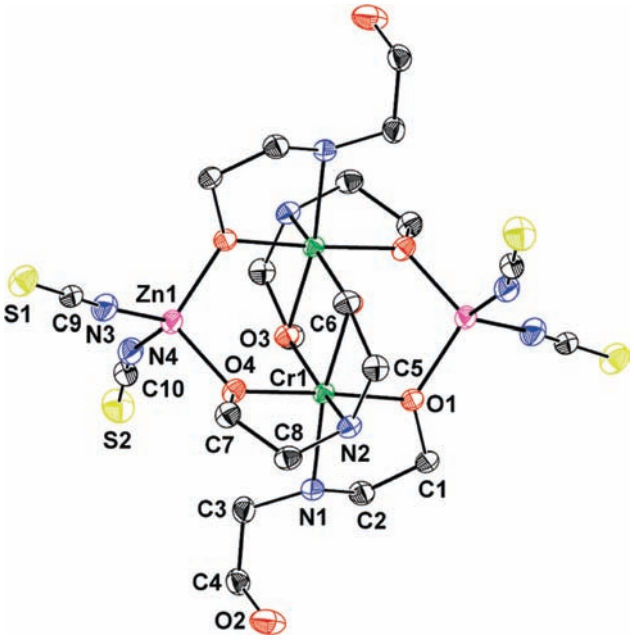


**Figure 1.** Molecular structure of **1** showing the atom numbering with 60% probability displacement ellipsoids. H atoms were omitted for clarity.

**Table 2.** Selected Bond Distances (Å) and Angles (deg) for **1** and **2**

| | **1** | **2** |
|---|---|---|
| Zn1−O1 | 1.967(2) | 1.968(3) |
| Zn1−O4 | 1.954(2) | 1.949(3) |
| Zn1−N3 | 1.968(3) | 1.949(3) |
| Zn1−N4 | 1.957(2) | 1.954(2) |
| Cr1−O1$^a$ | 1.966(2) | 1.964(2) |
| Cr1−O2$^a$ | 1.977(2) | 1.972(3) |
| Cr1−O2$^b$ | 1.987(2) | 1.974(3) |
| Cr1−O4$^b$ | 1.945(2) | 1.935(2) |
| Cr1−N1 | 2.072(3) | 2.075(3) |
| Cr1−N2 | 2.095(2) | 2.092(2) |
| | | |
| O1$^1$−Cr1−O2$^b$ | 86.98(7) | 87.68(6) |
| O1$^1$−Cr1−N1 | 81.92(7) | 81.88(7) |
| O1$^1$−Cr1−N2 | 94.40(7) | 95.75(7) |
| O2$^1$−Cr1−O2$^b$ | 81.02(7) | 80.66(7) |
| O2$^1$−Cr1−N1 | 84.39(7) | 84.36(7) |
| O2$^2$−Cr1−N1 | 160.78(6) | 161.01(8) |
| O2$^1$−Cr1−N2 | 170.19(6) | 169.84(7) |
| O2$^2$−Cr1−N2 | 102.05(7) | 100.73(8) |
| O4$^2$−Cr1−O1$^a$ | 177.10(6) | 176.43(7) |
| O4$^2$−Cr1−O2$^a$ | 87.64(6) | 87.16(7) |
| O4$^2$−Cr1−O2$^b$ | 94.46(7) | 95.75(7) |
| O4$^2$−Cr1−N1 | 97.37(7) | 95.09(8) |
| O4$^2$−Cr1−N2 | 82.85(7) | 82.68(7) |
| N1−Cr1−N2 | 94.43(8) | 96.09(8) |

$^a$ Symmetry operations for **1**: $-x, -y, -z$. $^b$ Symmetry operations for **2**: $1 - x, -y, 1 - z$.

(14) Sheldrick, G. M. *Acta Crystallogr.* **2008**, *A64*, 112–122.
(15) Nakamoto, K. *Infrared and Raman Spectra of Inorganic and Coordination Compounds*, 4th ed.; Wiley: New York, 1986.
(16) Wright, D. A.; Williams, D. A. *Acta Crystallogr.* **1968**, *B24*, 1107–1114.

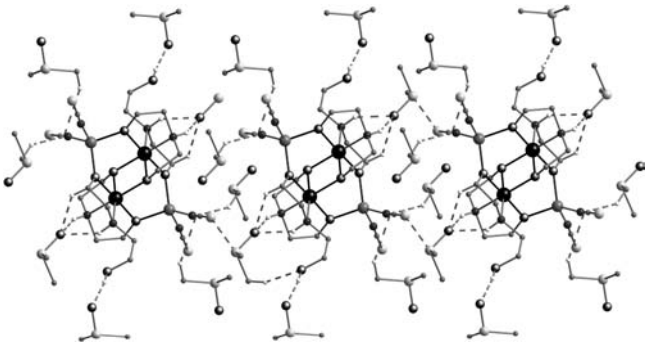

**Figure 2.** Fragment of the supramolecular chain in **1**.

ligands serve as $\mu_2$ bridges between two Cr atoms or between the Cr and Zn atoms, while only one O atom of the HDea ligand is coordinated to metals as a $\mu_2$ bridge between Cr and Zn atoms. The N atoms of both Dea and HDea are coordinated only to Cr.

In spite of the similarity of the molecules of **1** and **2**, their supramolecular architectures are quite different. In **1** (Figure 2), each tetranuclear aggregate is surrounded by 8 DMSO molecules bound by various types of hydrogen bonds. Two solvent molecules are bonded by the two N−H···O and one C−H···O hydrogen bond formed by the S3−O5 group of DMSO (N1−H3···O5, H···O 2.04 Å, N−H···O 146°; N2−H1···O5, H···O 2.13 Å, N−H···O 148°; C8−H8A···O5, H···O 2.47 Å, C−H···O 121°). It is interesting that three hydrogen bonds formed by the O atom of DMSO have a pyramidal configuration. The C12−S3−O5···H torsion angles are −52°, 67°, and −145°, respectively. A similar orientation of the hydrogen bonds was observed in a polyhydrated cytosine complex, where the carbonyl group has clearly enolic character, with the O atom of the C−O$^-$ bond containing three lone pairs.[17] Therefore, the presence of such a hydrogen-bond pattern reflects the high polarity and partial ionic character of the S−O bond of DMSO, as was previously demonstrated for sulfoxides.[18] These DMSO molecules, together with two other solvent molecules, are bonded also by the O−H···O and C−H···O hydrogen bonds to the noncoordinated hydroxy groups of the HDea ligands (O3−H3A···O6′ (−1 − *x*, −*y*, −1 − *z*), H···O 1.78 Å, O−H···O 167°; C12−H12C···O3, H···O 2.47 Å, C−H···O 153°].

Four other DMSO molecules are bound to the N4−C10−S2 isotiocyanate ligands. Two of them form the C−H···$\pi$ bonds to the $\pi$ system of that ligand (C−H···N 137°; C13−H13C···$\pi$(N4), H···N4 2.65 Å, C−H···N 149°; C14−H14B···$\pi$(C10), H···C10 2.76 Å, C−H···C 153°). The $\pi$ character of these hydrogen bonds is confirmed by the near-orthogonal location of the H atoms with respect to the almost linear ligand (the C−N···H and N−C···H angles are 92° and 65°, respectively). Two DMSO molecules are bonded to these ligands by a $\sigma$-hole or chalcogen bond[19,20] formed between the S atoms of ligand and DMSO molecules. The distance between the S2 and S3 atoms of 3.57 Å (while the van der Waals radii sum is 3.68 Å[21]) and the C11−S3···S2 angle of 150.2° clearly indicate that the lone pair of the S2 atom is oriented toward the area of positive electrostatic potential ($\sigma$-hole), which is located around the S3 atom as a continuation of the C11−S3 bond.

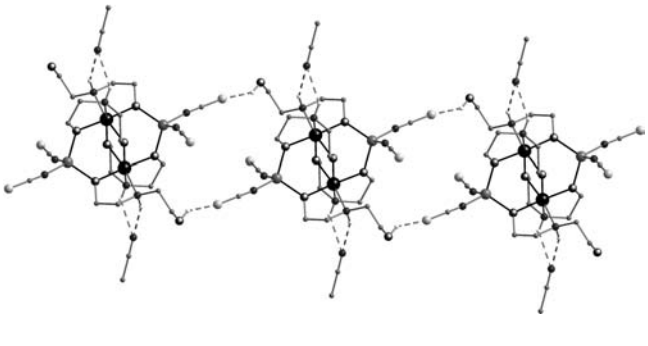

**Figure 3.** Fragment of the hydrogen-bonded chain in **2**.

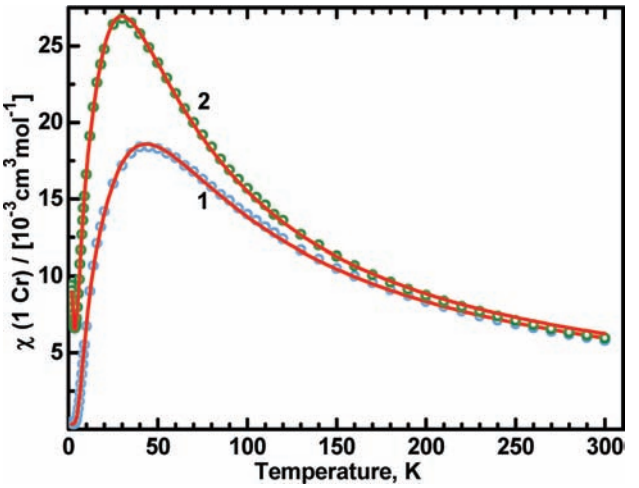


**Figure 4.** Magnetic susceptibility of **1** and **2**. Circles: experimental. Solid lines: calculated with $J = 13.7\ \text{cm}^{-1}$, $j = 1.12\ \text{cm}^{-1}$, $g = 1.983$, $f = 0$, and TIP $= 362 \times 10^{-6}$ cgs emu for **1** and $J = 9.4\ \text{cm}^{-1}$, $j = 0.83\ \text{cm}^{-1}$, $g = 1.983$, $f = 0.0095$, and TIP $= 474 \times 10^{-6}$ cgs emu for **2**. The factor to convert the molar susceptibility from cgs emu to SI units is $4\pi \times 10^{-6}$.

In **1**, the tetranuclear molecules form infinite chains (Figure 2) along the [110] direction, resulting from the C−H···$\pi$ hydrogen bonds between the DMSO molecule of one solvated complex and the isothiocyanate ligand N4−C10−S2 of a neighboring complex (C11−H11C···$\pi$(N4), H···N(4) 2.69 Å, C−N···H 111°).

In **2**, the solvent molecules do not act as bridges between neighboring complexes. They are bound to the complex by weak N−H···N hydrogen bonds (N1−H1N···N5, N···H 2.49 Å, N−H···N 139°; N2−H2N···N5, N···H 2.28 Å, N−H···N 154°]. The complexes arrange in infinite chains along the [101] direction (Figure 3), consisting of centrosymmetric dimers formed by means of the O−H···S hydrogen bonds O3−H3O···S2′ [(−*x*, 2 − *y*, −*z*) H···S 2.50 Å, O−H···S 145°].

**Magnetic Properties.** Magnetic susceptibility data of powdered samples are displayed in Figure 4. The effective magnetic moments of both complexes decrease when the temperature is lowered, indicating antiferromagnetic spin coupling between two $Cr^{III}$ $S = {}^3/_2$ centers. The

(17) Shishkin, O. V.; Gorb, L.; Leszczynski, J. *J. Phys. Chem.* **2000**, *A 104*, 5357–5361.
(18) Cioslowsky, J.; Surjan, P. R. *THEOCHEM* **1992**, *225*, 9–33.
(19) Politzer, P.; Murray, J. S.; Concha, M. C. *J. Mol. Model.* **2008**, *14*, 659–665.
(20) Wang, W.; Ji, B.; Zhang, Y. *J. Phys. Chem.* **2009**, *A 113*, 8132–8135.
(21) Zefirov, Yu. V.; Zorky, P. M. *Usp. Khim.* **1995**, *64*, 446–460.

intramolecular Cr−Cr distance is 3.01 Å in both **1** and **2**, while the shortest intermolecular Cr−Cr distances are 8.45 Å in **1** and 7.01 Å in **2**. The intermolecular interactions are thus unlikely to affect the magnetic susceptibility. Exchange interactions between two $S = {}^3/_2$ ions give rise to four states of the coupled spin $\hat{\boldsymbol{S}} = \hat{\boldsymbol{S}}_1 + \hat{\boldsymbol{S}}_2$, with the total $S$ quantum numbers 0, 1, 2, and 3, of which the state $S = 0$ is the lowest in energy. The magnetic properties of such dimeric systems are usually described by the HDVV Hamiltonian $\boldsymbol{H} = J\,\hat{\boldsymbol{S}}_1 \cdot \hat{\boldsymbol{S}}_2$. However, in our case, attempts to fit the magnetic susceptibility by using this Hamiltonian were unsuccessful, indicating a need for inclusion of the biquadratic exchange term that has often been applied to binuclear chromium(III) complexes and interacting chromium(III) pairs.[22]

$$\hat{H} = J\hat{\boldsymbol{S}}_1 \cdot \hat{\boldsymbol{S}}_2 - j(\hat{\boldsymbol{S}}_1 \cdot \hat{\boldsymbol{S}}_2)^2 \qquad (1)$$

An excellent fit over the entire temperature range 1.8−300 K was achieved using Hamiltonian (1). Figure S1 in the Supporting Information demonstrates the necessity of the biquadratic term.

The biquadratic exchange alters the usual Lande's interval rule $E_S - E_{S-1} = JS$ to $E_S - E_{S-1} = JS - jS\{S^2 - 2S_i(S_i + 1)\}$, where $S$ is a spin state of the coupled system (0, 1, 2, and 3) and $S_i$ ($i = 1$ or 2) is the spin of a single $Cr^{3+}$ ion ($^3/_2$). The magnetic susceptibility per one Cr atom can be calculated from

$$\chi_d = \frac{1}{2}\frac{Ng^2\mu_B{}^2}{3kT}\frac{\sum_{S=1}^{3}(2S+1)(S+1)S\exp(-E_S/kT)}{\sum_{S=0}^{3}(2S+1)\exp(-E_S/kT)} + \mathrm{TIP} \qquad (2)$$

$$\text{with } E_S = J\{S(S+1) - 15/2\}/2 - j\{S(S+1) - 15/2\}^2/4 \qquad (3)$$

A contribution due to paramagnetic contamination was seen at the lowest temperatures in **2** but much less so in **1**. Assuming that it is due to a monomeric chromium(III) species whose fraction is $f$, the susceptibility can be expressed as

$$\chi_{total} = (1-f)\chi_d + f\chi_{mono} \qquad (4)$$

$$\chi_{mono} = -\frac{Ng\mu_B}{B}\frac{\sum_{m=-3/2}^{3/2} m\exp(-g\mu_B mB/kT)}{\sum_{m=-3/2}^{3/2}\exp(-g\mu_B mB/kT)} + \mathrm{TIP} \qquad (5)$$

In 5, $B$ is the magnetic induction of the magnetometer (0.5 T). Using the Curie law to calculate the monomer susceptibility at the lowest temperatures would not be appropriate because the Zeeman splitting (~0.47 $cm^{-1}$ at 0.5 T) is comparable to $kT$ (1.4 $cm^{-1}$ at 2 K). The temperature-independent paramagnetism (TIP) was assumed to be the same for $Cr^{III}$ in both the dimer and the monomeric impurity. While TIP has not been taken into account by many researchers who interpreted the magnetic properties of chromium(III) complexes,[23] it appears not to be negligible and magnitudes on the order of (100−300) × $10^{-6}$ cgs em units per one Cr atom are typically found[24] in agreement with theoretical estimations.[24d] TIP as high as 800 × $10^{-6}$ emu was found in simple chromium(III) salts.[24e]

When $g$ was fixed at its EPR value of 1.983, the following parameters were found: $J$ = 13.7(1) $cm^{-1}$, $j$ = 1.12(1) $cm^{-1}$, $f$ = 0(5) × $10^{-6}$, and TIP = 362(22) × $10^{-6}$ cgs emu for **1** and $J$ = 9.4(1) $cm^{-1}$, $j$ = 0.83(1) $cm^{-1}$, $f$ = 0.0095(1), and TIP = 474(35) × $10^{-6}$ cgs emu for **2**. The TIP values, while high, appear to be still acceptable. On the other hand, if TIP was set to zero, the best-fit parameters were $J$ = 14.6(1) $cm^{-1}$, $j$ = 0.98(1) $cm^{-1}$, $g$ = 2.036(1), and $f$ = 0.00049(2) for **1** and $J$ = 10.0(1) $cm^{-1}$, $j$ = 0.75(2) $cm^{-1}$, $g$ = 2.030(5), and $f$ = 0.0094(1) for **2**. Neglecting TIP would not cause major errors in $J$ and $j$ because the magnetic susceptibility of our compounds is large; however, the resulting $g$ values are too high; they should be smaller than 2 for $Cr^{3+}$. A too high $g$ value (2.03) was also reported in ref 25, possibly caused by neglect of TIP.

The biquadratic exchange term was introduced in the 1960s[22d−h,26] to explain the temperature variation of the EPR spectra intensity due to pairs of $Mn^{2+}$ or $Cr^{3+}$ ions. The most important contribution to the $j$ parameter is thought to be the "exchange striction", which is the exchange interaction effect on the equilibrium distance $R_T$ between metal ions in a lattice.[22d−h,26] $j$ depends on the elastic stiffness coefficient $c$. In the spinel $MgAl_2O_4$ doped with $Cr^{3+}$, in which $J$ equals 22 $cm^{-1}$, $j$ = 1.7 $cm^{-1}$ was experimentally determined and was excellently reproduced by the formula $j = (1/2)(dJ/dR_T)^2 cR_T$.[22d,f] In the sign convention used in the present paper, the exchange striction results in positive $j$, in agreement with our results above. The exchange striction is considered to be of paramount importance in cases of 90° Cr−O−Cr interactions,[22d,e] while in our case, the angles are about 99°. Similar $j$ values were found in other $Cr^{3+}$-doped spinels,

(22) (a) Fischer, H. R.; Glerup, J.; Hodgson, D. J.; Pedersen, E. *Inorg. Chem.* **1982**, *21*, 3063–3066. (b) Cline, S. J.; Hodgson, D. J.; Kallesoe, S.; Larsen, S.; Pedersen, E. *Inorg. Chem.* **1983**, *22*, 631–642. (c) Scaringe, R. P.; Singh, P.; Eckberg, R. P.; Hatfield, W. E.; Hodgson, D. J. *Inorg. Chem.* **1975**, *14*, 1127–1133. (d) Henning, J. C. M.; den Boef, J. H.; van Gorkom, G. C. P. *Phys. Rev. B* **1973**, *7*, 1825–1833. (e) Henning, J. C. M.; Damen, J. P. M. *Phys. Rev. B* **1971**, *3*, 3852–3854. (f) Henning, J. C. M.; van den Boom, H. *Phys. Rev. B* **1973**, *8*, 2255–2262. (g) Gutowski, M. *Phys. Rev. B* **1978**, *18*, 5984–5989. (h) Ikeda, H.; Kimura, I.; Uryu, N. *J. Chem. Phys.* **1968**, *48*, 4800–4800. (i) Ciornea, V.; Mingalieva, L.; Costes, J. P.; Novitchi, G.; Filippova, I.; Galeev, R. T.; Shova, S.; Voronkova, V. K.; Gulea, A. *Inorg. Chim. Acta* **2008**, *361*, 1947–1957. (j) Kremer, S. *Inorg. Chem.* **1985**, *24*, 887–890.

(23) (a) Brudenell, S. J.; Crimp, S. J.; Higgs, J. K. E.; Moubaraki, B.; Murray, K. S.; Spiccia, L. *Inorg. Chim. Acta* **1996**, *247*, 35–41. (b) Glerup, J.; Goodson, P. A.; Hodgson, D. J.; Massod, M. A.; Michelsen, K. *Inorg. Chim. Acta* **2005**, *358*, 295–302. (c) Glerup, J.; Weihe, H. *Inorg. Chem.* **1997**, *36*, 2816–2819.

(24) (a) Vlachos, A.; Psycharis, V.; Raptopoulou, C. P.; Lalioti, N.; Sanakis, Y.; Diamantopoulos, G.; Fardis, M.; Karayanni, M.; Papavassiliou, G.; Terzis, A. *Inorg. Chim. Acta* **2004**, *357*, 3162–3172. (b) Figuerola, A.; Tangoulis, V.; Ribas, J.; Hartl, H.; Brüdgam, I.; Maestro, M.; Diaz, C. *Inorg. Chem.* **2007**, *46*, 11017–11024. (c) Cavell, R. G.; Byers, W.; Day, E. D. *Inorg. Chem.* **1971**, *10*, 2710–2715. (d) Boča, R. *Struct. Bonding (Berlin)* **2006**, *117*, 1–264. (e) Vucinic, M.; Mitric, M.; Kusigerski, V.; Kapor, A.; Szytula, A. *J. Res. Phys.* **2002**, *29*, 79–83.

(25) Burdinski, D.; Bill, E.; Birkelbach, F.; Wieghardt, K.; Chaudhuri, P. *Inorg. Chem.* **2001**, *40*, 1160–1166.

(26) (a) Kittel, C. *Phys. Rev.* **1960**, *120*, 335–342. (b) Harris, E. A.; Owen, J. *Phys. Rev. Lett.* **1963**, *11*, 9–10. (c) Rodbell, D. S.; Jacobs, I. S.; Owen, J.; Harris, E. A. *Phys. Rev. Lett.* **1963**, 10–12.

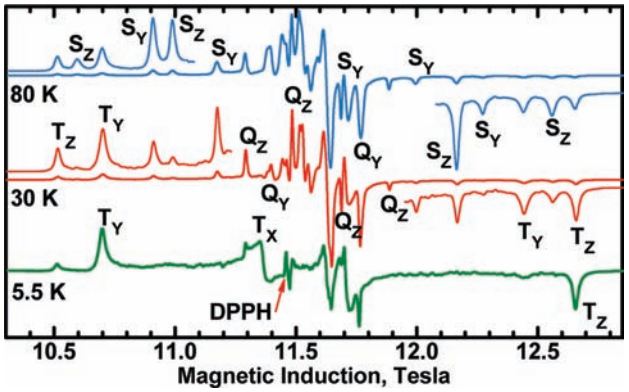


**Figure 5.** Powder EPR spectra of **1** at 321.6 GHz at the temperatures indicated. The temperature dependencies allow assign transitions to the triplet, quintet, and septet spin states ($S = 1-3$, marked with T, Q, and S, respectively) and determine the sign of the zfs parameters in each spin state (Table 3). X, Y, and Z indicate the molecular orientations for respective resonances. The spin Hamiltonian parameters changed insignificantly between 80 and 5.5 K.

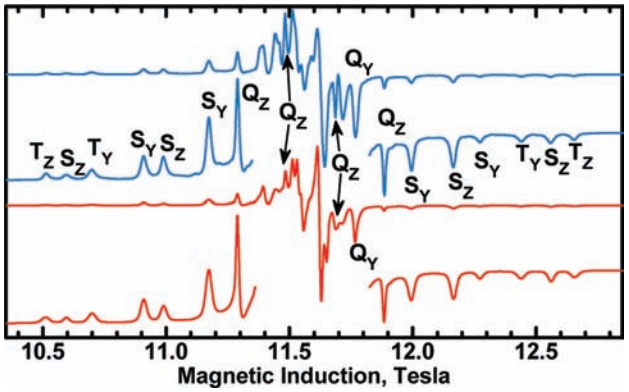


**Figure 6.** EPR spectra of **1** at 321.6 GHz and 80 K. Top: Experimental spectrum. Bottom: Spectrum simulated with $J = 13.7\ cm^{-1}$, $j = 1.1\ cm^{-1}$, $D_{Cr} = 0.3864\ cm^{-1}$, $E_{Cr} = -0.1104\ cm^{-1}$, $D_{12} = -0.1873\ cm^{-1}$, and $E_{12} = -0.0155\ cm^{-1}$. Resonances are labeled as in Figure 5. The simulation procedure is described in the text. The wings of the experimental and simulated spectra are magnified 4.5 and 10 times, respectively.

for example, $J = 11\ cm^{-1}$ and $j = 1.7\ cm^{-1}$ in $ZnGa_2O_4$,[22e] and the $j$ magnitudes over a wide range have also been reported for complexes with organic ligands, like $j = 0.1\ cm^{-1}$ ($J = 9.4\ cm^{-1}$) in $[(acac)_2Cr(OCH_3)]_2$,[22a] $j = 1.5\ cm^{-1}$ ($J = 44\ cm^{-1}$) in $[Cr(phen)_2(OH)]_2I_4(H_2O)_4$,[22c] and $j = 4.9\ cm^{-1}$ ($J = 30\ cm^{-1}$) in $[Ba(H_2O)_4Cr_2(OH)_2(nta)_2]\cdot 3H_2O$.[22i]

Finally, it should be mentioned that there is no significant effect on the magnetic susceptibility due to the zero-field splitting (zfs) in the spin states $S = 1-3$. This was checked by applying Hamiltonian (6) (see the EPR Spectra section) to calculate the magnetic susceptibility with and without zfs (Figure S4 in the Supporting Information). The zfs effect can only be observed in ferromagnetic dimeric or polymeric systems, at low temperatures where only a ground state with $S \geq 1$ is populated.[27b] The magnetic susceptibility of antiferromagnetic systems approaches zero with the temperature decreasing before the zfs can become important. In the present systems, the zfs parameter $D$ in $S = 1$ is of a magnitude similar to that of $j$. However, the relative strength of the $D$ effect is an order of magnitude smaller than that of $j$ because the triplet

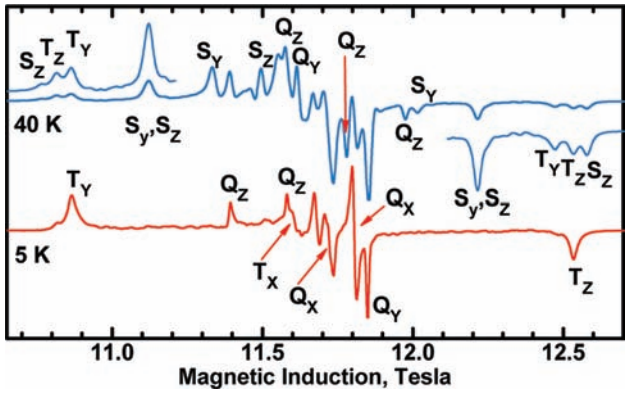


**Figure 7.** EPR spectra of **2** at 324.0 GHz at the temperatures indicated. Resonances are labeled as in Figure 5. The temperature dependencies allow one to assign transitions to the respective spin states and determine the sign of the zfs parameters in each state.

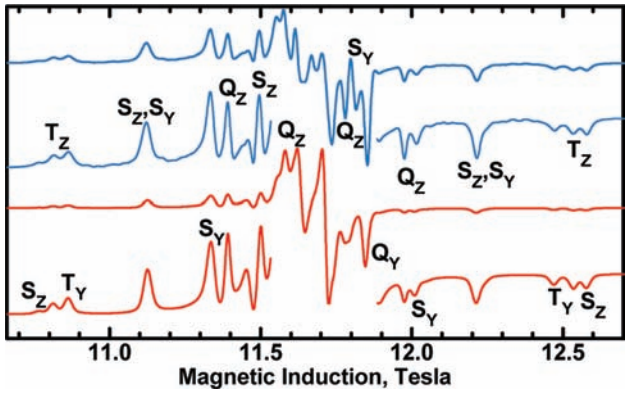


**Figure 8.** EPR spectra of **2** at 324.0 GHz and 40 K. Top: Experimental spectrum. Bottom: Simulated with $J = 9.4\ cm^{-1}$, $j = 0.83\ cm^{-1}$, $D_{Cr} = 0.3564\ cm^{-1}$, $E_{Cr} = -0.0647\ cm^{-1}$, $D_{12} = -0.1850\ cm^{-1}$, and $E_{12} = -0.0112\ cm^{-1}$. Resonances are labeled as in Figure 5.

sublevel energies (with respect to the singlet ground state) are $J - 6.5j + D/3 \pm g\mu_B B$ (for $M_S = \pm 1$) and $J - 6.5j - 2D/3$ (for $M_S = 0$).

**EPR Spectra.** Both complexes exhibited very well-resolved high-frequency EPR spectra in which resonances due to spin states $S = 1-3$ were observed (see Figures 5−8). Complex **1** showed well-resolved X-band spectra with only $S = 2$ resonances visible below 0.7 T (Figure 9), similarly to other reports,[22i,j,23c,d,25] while lines due to the $S = 1$ and 3 states could be observed at higher field. Only a broad, poorly resolved X-band spectrum of **2** could be seen. The spin states $S = 1$ and 3 are difficult to observe in the X-band EPR because the zfs in these states is much larger than that in the $S = 2$ state and may be too large compared to the X-band quantum energy. Because the antiferromagnetic interactions in the present two systems are weak, EPR spectra could be observed at very low temperatures, making possible the sign determination of the zfs parameters in each spin state.

The sign determination relies on the intensity ratios of the low- and high-field halves of the EPR spectra and requires that the Zeeman splitting be comparable to the thermal energy $kT$. This is easily achievable in high-frequency EPR at low temperatures.[27]

Knowledge of the sign of the zfs parameters is crucial for evaluation of the contributions due to the Cr−Cr

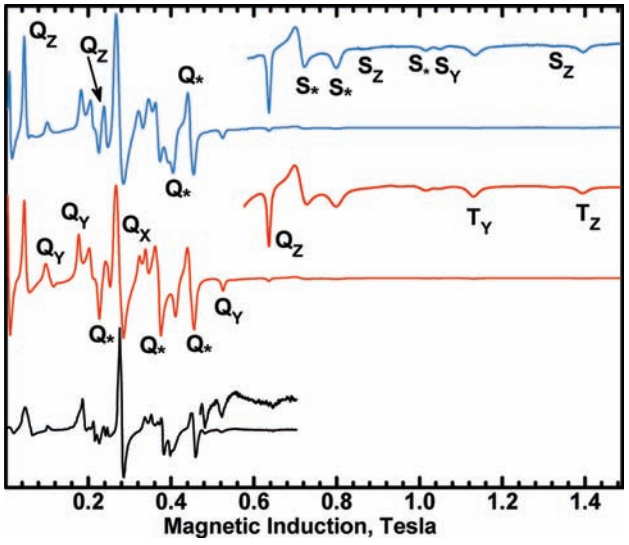


**Figure 9.** X-band EPR spectra of **1**. Top: Experimental spectrum of a powder sample at 9.396 GHz and 40 K. Center: Simulation with parameters given in the Figure 6 caption. Some prominent off-axial turning points are marked with asterisks. Bottom: Frozen DMF solution (9.64 GHz and 77 K). The polynuclear molecule appears to be retained in a DMF solution. Essentially, only the quintet state ($S = 2$) contributes to the X-band spectra below 0.65 T.

interactions and to the zfs on individual Cr ions (below). The EPR parameters in Table 3 were found by spectra simulations using Hamiltonian (10) (see the Interpretation of the EPR Spectra section), with the zfs parameters $D$ and $E$ being different in each spin state. Although Hamiltonians (7) and (10) are not strictly correct in the present case, where the exchange interactions are relatively weak, the parameters in Table 3 serve as a very good starting point for a more rigorous treatment (see below).

The microwave frequencies and magnetic fields used in this work are high enough to induce transitions between different spin states (Figure S2 in the Supporting Information), like between triplet and quintet states. However, such transitions are strongly forbidden in centrosymmetric dimers,[28] and, accordingly, no indication of such resonances was observed.

**Interpretation of the EPR Spectra.** The spin Hamiltonian operator appropriate to our binuclear systems is

$$\hat{H} = J\hat{\boldsymbol{S}}_1\cdot\hat{\boldsymbol{S}}_2 - j(\hat{\boldsymbol{S}}_1\cdot\hat{\boldsymbol{S}}_2)^2 + \mu_B\boldsymbol{B}\{g_1\}\hat{\boldsymbol{S}}_1 + \hat{\boldsymbol{S}}_1\{D_1\}\hat{\boldsymbol{S}}_1 + \mu_B\boldsymbol{B}\{g_2\}\hat{\boldsymbol{S}}_2 + \hat{\boldsymbol{S}}_2\{D_2\}\hat{\boldsymbol{S}}_2 + \hat{\boldsymbol{S}}_1\{D_{12}\}\hat{\boldsymbol{S}}_2 \quad (6)$$

where the individual terms refer to the isotropic bilinear and biquadratic exchanges, the local Zeeman and single-ion anisotropy terms, which are parametrized by the $\{g_1\}$, $\{g_2\}$ and $\{D_1\}$, $\{D_2\}$ tensors, respectively, and the $\{D_{12}\}$ term that contains the magnetic dipolar interactions along with the anisotropic exchange. In our case, $\{D_1\} = \{D_2\} = \{D_{Cr}\}$. In the strong exchange limit (isotropic interactions much stronger than the zfs effects), the Hamiltonian may be conveniently expressed by using the total spin operator, $\hat{\boldsymbol{S}} = \hat{\boldsymbol{S}}_1 + \hat{\boldsymbol{S}}_2$. After removal of the $J$ and $j$ terms of eq 6, which do not affect the resonance fields in EPR spectra, one can write for each spin state $S$

$$\hat{H}_S = \mu_B\boldsymbol{B}\cdot\{g_S\}\cdot\hat{\boldsymbol{S}} + \hat{\boldsymbol{S}}\cdot\{D_S\}\cdot\hat{\boldsymbol{S}} \quad (7)$$

where the $\{g_S\}$ and $\{D_S\}$ tensors are different in each spin state. In particular, the $\{D_S\}$ tensors in different spin states are not, in general, coaxial, which can be seen in single-crystal EPR.[29] The transition from Hamiltonian (6) to (7) is accomplished by using coefficients $\alpha_S$ and $\beta_S$, which can be found in many texts.[30]

$$\{D_S\} = \alpha_S\{D_{12}\} + \beta_S(\{D_1\} + \{D_2\}) \quad (8)$$

where

$$\alpha_S = [S(S+1) + 2S_1(S_1+1) + 2S_2(S_2+1)]/[2(2S-1)(2S+3)]$$
$$\beta_S = [3S(S+1) - 2S_1(S_1+1) - 2S_2(S_2+1) - 3]/[2(2S-1)(2S+3)] \quad (9)$$

In both eqs 6 and 7, the $\{D\}$ tensor components may be replaced by the $D$ and $E$ parameters if a system of coordinates has been found in which the respective tensors are diagonal. Thus, eq 7 can be converted to eq 10:

$$\hat{H}_S = \mu_B\boldsymbol{B}\cdot\{g_S\}\cdot\hat{\boldsymbol{S}} + D_S\{\hat{\boldsymbol{S}}_z^2 - S(S+1)/3\} + E_S(\hat{\boldsymbol{S}}_x^2 - \hat{\boldsymbol{S}}_y^2) \quad (10)$$

**Table 3.** EPR Parameters in the Spin States 1−3 for Complexes **1** and **2** Obtained from Simulations Using Hamiltonian (10)

| spin $S$ | $g_x$ | $g_y$ | $g_z$ | $D$, cm$^{-1}$ | $E$, cm$^{-1}$ |
|---|---|---|---|---|---|
| | | | Complex **1** | | |
| 1 | 1.983 | 1.985 | 1.983 | 0.9908 | 0.2076 |
| 2 | 1.982 | 1.984 | 1.983 | −0.0919 | −0.0079 |
| 3 | 1.983 | 1.983 | 1.984 | 0.1819 | 0.0237 |
| | | | Complex **2** | | |
| 1 | 1.980 | 1.983 | 1.983 | 0.7964 | 0.2309 |
| 2 | 1.981 | 1.983 | 1.982 | −0.0908 | −0.0056 |
| 3 | 1.982 | 1.982 | 1.983 | 0.1678 | 0.0131 |

(27) (a) Ozarowski, A. *Inorg. Chem.* **2008**, *47*, 9760–9762. (b) Ozarowski, A.; Szymanska, I. B.; Muziol, T.; Jezierska, J. *J. Am. Chem. Soc.* **2009**, *131*, 10279–10292. (c) Makhankova, V. G.; Beznischenko, A. O.; Kokozay, V. N.; Zubatyuk, R. I.; Shishkin, O. V.; Jezierska, J.; Ozarowski, A. *Inorg. Chem.* **2008**, *47*, 4554–4563. (d) Herchel, R.; Boča, R.; Krzystek, J.; Ozarowski, A.; Duran, M.; van Slageren, J. *J. Am. Chem. Soc.* **2007**, *129*, 10306–10307. (e) Aromi, G.; Telser, J.; Ozarowski, A.; Brunel, L. C.; Stoeckli-Evans, H. M.; Krzystek, J. *Inorg. Chem.* **2005**, *44*, 187–196. (f) Ozarowski, A.; Zvyagin, S. A.; Reiff, W. M.; Telser, J.; Brunel, L. C.; Krzystek, J. *J. Am. Chem. Soc.* **2004**, *126*, 6574–6575. (g) Krzystek, J.; Zvyagin, S. A.; Ozarowski, A.; Fiedler, A. T.; Brunold, T. C.; Telser, J. *J. Am. Chem. Soc.* **2004**, *126*, 2148–2155.

(28) Carr, S. G.; Smith, T. D.; Pilbrow, J. R. *J. Chem. Soc., Faraday Trans. 2*, **1974**, *70*, 497−511 and Supplementary Publication SUP20897, *J. Chem. Soc., Faraday Trans. 2* **1974**.

(29) (a) Ozarowski, A.; McGarvey, B. R.; Drake, J. E. *Inorg. Chem.* **1995**, *34*, 5558–5566. (b) Holgate, S. J.; Bondarenko, G.; Collison, D.; Mabbs, F. E. *Inorg. Chem.* **1999**, *38*, 2380–2385. (c) ter Heerdt, P.; Stefan, M.; Goovaerts, E.; Caneschi, A.; Cornia, A. *J. Magn. Reson.* **2006**, *179*, 29–37.

(30) (a) Owen, J. *J. Appl. Phys.* **1961**, *32*, 213S–217S. (b) Abragam, A.; Bleaney, B. *Electron Spin Resonance of Transition Ions*; Clarendon Press: London, 1970. (c) Bencini, A.; Gatteschi, D. *EPR of Exchange Coupled Systems*; Springer-Verlag: Berlin, 1990. (d) Okamura, M. Y.; Hoffman., B. M. *J. Chem. Phys.* **1969**, *51*, 3128–3129. (e) Boča, R. *Theoretical Foundations of Molecular Magnetism*; Elsevier: Amsterdam, The Netherlands, 1999. (f) Boča, R. *Coord. Chem. Rev.* **2004**, *248*, 757–815.

The relationships between the scalar $D$ and $E$ parameters of eq 10 and the $\{D\}$ tensor components are

$$D = (2D_{zz} - D_{xx} - D_{yy})/2; \quad E = (D_{xx} - D_{yy})/2$$
$$D_{zz} = (2/3)D; \; D_{xx} = -(D/3) + E; \; D_{yy} = -(D/3) - E \tag{11}$$

Similarly, eq 6, with the $J$- and $j$-containing terms removed, can be converted to eq 12:

$$\begin{aligned}\hat{\mathrm{H}} &= \mu_{\mathrm{B}}\boldsymbol{B}\{g_1\}\hat{\boldsymbol{S}}_1 + D_1\{\hat{\boldsymbol{S}}_{z1}^2 - S_1(S_1+1)/3\} \\ &+ E_1(\hat{\boldsymbol{S}}_{x1}^2 - \hat{\boldsymbol{S}}_{y1}^2) + \mu_{\mathrm{B}}\boldsymbol{B}\{g_2\}\hat{\boldsymbol{S}}_2 + D_2\{\hat{\boldsymbol{S}}_{z2}^2 \\ &- S_2(S_2+1)/3\} + E_2(\hat{\boldsymbol{S}}_{x2}^2 - \hat{\boldsymbol{S}}_{y2}^2) + D_{12}\{\hat{\boldsymbol{S}}_{z1}\hat{\boldsymbol{S}}_{z2} \\ &- \hat{\boldsymbol{S}}_1\cdot\hat{\boldsymbol{S}}_2/3\} + E_{12}(\hat{\boldsymbol{S}}_{x1}\hat{\boldsymbol{S}}_{x2} - \hat{\boldsymbol{S}}_{y1}\hat{\boldsymbol{S}}_{y2})\end{aligned} \tag{12}$$

In this notation, relationships (11) are valid for all $\{D_1\}$, $\{D_2\}$, and $\{D_{12}\}$ tensors, and relationships (8) and (9) can be applied to both the tensors and the scalar parameters $D$ and $E$. This cannot be done if the $D_{12}$ term in eq 12 is written as $D_{12}\{2\hat{\boldsymbol{S}}_{z1}\hat{\boldsymbol{S}}_{z2} - \hat{\boldsymbol{S}}_{x1}\hat{\boldsymbol{S}}_{x2} - \hat{\boldsymbol{S}}_{y1}\hat{\boldsymbol{S}}_{y2}\}$, which is equivalent to $D_{12}\{3\hat{\boldsymbol{S}}_{z1}\hat{\boldsymbol{S}}_{z2} - \hat{\boldsymbol{S}}_1\cdot\hat{\boldsymbol{S}}_2\}$.[22j,23c,d,30b,d]

In a binuclear chromium(III) complex, the coefficients are $\alpha_1 = 1.7$, $\alpha_2 = 0.5$, $\alpha_3 = 0.3$, $\beta_1 = -1.2$, $\beta_2 = 0$, and $\beta_3 = 0.2$, and because there are two equivalent Cr ions in the system, $\{D_1\} = \{D_2\} = \{D_{\mathrm{Cr}}\}$, and

$$\begin{aligned}\{D_{S=1}\} &= 1.7\{D_{12}\} - 2.4\{D_{\mathrm{Cr}}\} \\ \{D_{S=2}\} &= 0.5\{D_{12}\} \\ \{D_{S=3}\} &= 0.3\{D_{12}\} + 0.4\{D_{\mathrm{Cr}}\}\end{aligned} \tag{13}$$

The zfs on single CrIII ions (represented by $\{D_{\mathrm{Cr}}\}$) does not contribute to the zfs in the quintet state of a $^3/_2$–$^3/_2$ dimer (however, see below). Both the dipole–dipole and anisotropic exchange interactions contribute to the $\{D_{12}\}$ tensor:

$$\{D_{12}\} = \{D^{\mathrm{dipolar}}\} + \{D^{\mathrm{exchange}}\} \tag{14}$$

The dipolar part can be calculated from formulas in ref 28, which take very simple forms for our centrosymmetric dimers:

$$\begin{aligned}D_{xx}^{\mathrm{dipolar}} &= g_x^2\mu_{\mathrm{B}}^2/R^3 \\ D_{yy}^{\mathrm{dipolar}} &= g_x^2\mu_{\mathrm{B}}^2/R^3 \\ D_{zz}^{\mathrm{dipolar}} &= -2g_z^2\mu_{\mathrm{B}}^2/R^3\end{aligned} \tag{15}$$

Formulas (15) assume the $z$ axis along the Cr–Cr direction and are appropriate for Hamiltonian (6). In this context, it is noteworthy that the experimental zfs parameters in the quintet state of both **1** and **2** are very similar because they largely depend on the dipole–dipole interactions, and the Cr–Cr distances in **1** and **2** are practically equal. Formulas (8) and (13) are correct only when the isotropic exchange interactions are much stronger than the anisotropic interactions. Because this is not exactly the case here, the spin-state mixing may affect the spectra, and Hamiltonian (6) or its equivalent (eq 12) should be used rather than eq 7 or eq 10.[23c,d,25] "Spin-state mixing" occurs because the coupled spin states that are eigenfunctions of both $\hat{\boldsymbol{S}}^2$ and $J\,\hat{\boldsymbol{S}}_1\cdot\hat{\boldsymbol{S}}_2 - j(\hat{\boldsymbol{S}}_1\cdot\hat{\boldsymbol{S}}_2)^2$ are not eigenfunctions of a Hamiltonian with the zfs terms included. The importance of spin-state mixing can be assessed by simulating EPR spectra using Hamiltonian (6), first with the correct values of $J$ and $j$ and then repeating the simulations with $J$, $j$, and the temperature multiplied by 100, thus eliminating the spin-state mixing while maintaining the relative populations of the $S = 1$–3 levels (see Figure S3 in the Supporting Information). It is found that the effect causes shifts of the four allowed $S = 2$ lines at the $Z$ orientation by +0.0090, +0.0003, −0.0003, and −0.0036 T at 321.6 GHz and by +0.0047, 0, 0, and −0.0056 T at the X-band frequency in a pattern that may be confused with the presence of the fourth-order terms in the spin Hamiltonian, as was noted in ref 25. The resonance fields in the $S = 1$ and 3 states are virtually unaffected, with shifts smaller than 0.0012 T (out of the overall splitting of 2.14 T in $S = 1$). Also, the $S = 2$ spectra depend only weakly on $D_{\mathrm{Cr}}$ and $E_{\mathrm{Cr}}$. The challenge now is to find the $D_{\mathrm{Cr}}$, $E_{\mathrm{Cr}}$, $D_{12}$, and $E_{12}$ parameters that will satisfactorily simulate the observed spectra. This is not an easy task because the $\{D_{\mathrm{Cr}}\}$ and $\{D_{12}\}$ tensors need not be coaxial and no single-crystal spectra are available to help in the determination of their relative orientation. The behavior described above, the insensitivity of the EPR spectra for $S = 1$ and 3 to the spin-state mixing and the weak sensitivity of the $S = 2$ spectra to $D_{\mathrm{Cr}}$ and $E_{\mathrm{Cr}}$, suggests that one may determine $D_{12}$ and $E_{12}$ by analyzing the $S = 2$ component in the experimental EPR spectra using Hamiltonian (6), with $D_{\mathrm{Cr}}$ and $E_{\mathrm{Cr}}$ determined approximately from the zfs values in the $S = 1$ and 3 states, and subsequently refine $D_{\mathrm{Cr}}$ and $E_{\mathrm{Cr}}$. The initial magnitudes of $D_{\mathrm{Cr}}$ and $E_{\mathrm{Cr}}$ could be evaluated from data in Table 3.

Thus, for **1**, the three diagonal components of the $\{D_{S=1}\}$ and $\{D_{S=3}\}$ tensors were found from respective $D$ and $E$ parameters (Table 3) through formulas (11) and were aligned as shown below. Such an alignment (the diagonal components of $\{D_{S=1}\}$ and $\{D_{S=3}\}$ with the largest absolute values were assigned as $xx$ and $yy$, respectively) means that the respective tensors are assumed to be perpendicular to each other. Further, the $\{D_{\mathrm{Cr}}\}$ and $\{D_{12}\}$ components were calculated by using rearranged formulas (13):

| | $xx$ | $yy$ | $zz$ |
|---|---|---|---|
| $\{D_{S=1}\}$ | 0.6605 | −0.5378 | −0.1227 |
| $\{D_{S=3}\}$ | −0.0843 | 0.1213 | −0.037 |
| $\{D_{\mathrm{Cr}}\}$ | −0.2439 | 0.2625 | −0.0186 |
| $\{D_{12}\}$ | 0.0442 | 0.0543 | −0.0984 |

All data above are in $\mathrm{cm}^{-1}$. The tensor components in the lower two rows can be converted to the respective $D$ and $E$ parameters, resulting in $D_{\mathrm{Cr}} = 0.394\ \mathrm{cm}^{-1}$, $E_{\mathrm{Cr}} = -0.113\ \mathrm{cm}^{-1}$ and $D_{12} = -0.147\ \mathrm{cm}^{-1}$, $E_{12} = -0.005\ \mathrm{cm}^{-1}$ [for Hamiltonian (12). When the tensor components were converted to $D$ and $E$ parameters, the one with the largest absolute magnitude was taken as the $zz$ component. The resulting $\{D_{\mathrm{Cr}}\}$ and $\{D_{12}\}$ tensors are mutually perpendicular. An analogous procedure gave for **2** $D_{\mathrm{Cr}} = 0.364\ \mathrm{cm}^{-1}$, $E_{\mathrm{Cr}} = -0.076\ \mathrm{cm}^{-1}$, $D_{12} = -0.125\ \mathrm{cm}^{-1}$, and $E_{12} = -0.0083\ \mathrm{cm}^{-1}$. It will be shown below that while $D_{\mathrm{Cr}}$ and $E_{\mathrm{Cr}}$ obtained in this way are quite good, the values of $D_{12}$ and $E_{12}$ are incorrect mainly because of the above

assumption of $\{D_{S=1}\}$ and $\{D_{S=3}\}$ being exactly perpendicular to each other. Actually, taking simply $D_{12} = 2D_{S=2}$ and $E_{12} = 2E_{S=2}$ [see Table 3 and formulas (13)] offers a much better approximation.

Further, the following strategy was devised: (1) $D_{12}$ and $E_{12}$ were determined from the $S = 2$ resonances by using Hamiltonian (6) with the starting $D_{Cr}$ and $E_{Cr}$ magnitudes and were converted to the $\{D_{12}\}$ tensor. (2) New values of $D_{Cr}$ and $E_{Cr}$ were chosen and converted to the $\{D_{Cr}\}$ tensor (eq 11). (3) The $\{D_{Cr}\}$ tensor was transformed into the coordinates of $\{D_{12}\}$ by rotating it about the $x$, $y$, and $z$ axes by angles $\alpha$, $\beta$, and $\gamma$, respectively. (4) $\{D_{S=1}\}$ and $\{D_{S=3}\}$ tensors were evaluated according to formulas (13) and diagonalized. (5) $D_{S=1}$, $E_{S=1}$, $D_{S=3}$, and $E_{S=3}$ were evaluated from the diagonalized tensors (eq 11). The procedure was repeated until $D_{Cr}$ and $E_{Cr}$ and angles $\alpha$, $\beta$, and $\gamma$ were found, which resulted in the zfs parameters for $S = 1$ and 3 equal to those in Table 3, which were found before by using Hamiltonian (10) separately for the triplet and septet states. Angles $\alpha = 106.6°$, $\beta = 33.9°$, and $\gamma = 2.7°$ were needed for **1**, while $\alpha = 108.7°$, $\beta = 37.1°$, and $\gamma = 2.5°$ were found for **2**. The $D_{Cr}$, $E_{Cr}$, $D_{12}$, and $E_{12}$ parameters found in this way were 0.3864, −0.1104, −0.1873, and −0.0155 $cm^{-1}$, respectively, for **1**, and 0.3564, −0.0647, −0.1850, and −0.0112 $cm^{-1}$, respectively, for **2**. $D_{Cr}$ and $E_{Cr}$ did not change much from their seed values, and it is seen that the main question in this procedure is indeed finding the relative orientation of the tensors. Finally, EPR spectra for **1** and **2** were simulated with these parameter sets, taking into account the orientation of the $\{D_{Cr}\}$ tensor versus the $\{D_{12}\}$ tensor, given by the angles $\alpha$, $\beta$, and $\gamma$. The simulation program written by one of us was not trivial and deserves a description.

**Simulation of the EPR Spectra.** All calculations were performed in the axes of $\{D_{12}\}$, which are naturally related to the molecular geometry (assuming that $\{D_{12}\}$ is mainly of dipolar nature): the $z$ axis was the Cr−Cr vector and the $y$ axis was perpendicular to the $Cr_2O_2$ plane. The program used input the scalar parameters as $D_{Cr}$, $E_{Cr}$, $D_{12}$, and $E_{12}$, which were converted to the $\{D_{Cr}\}$ and $\{D_{12}\}$ tensors. The $\{g\}$ tensors were assumed to be coaxial with $\{D_{Cr}\}$. The $g$ anisotropy is very small (Table 3), yet it has a visible effect under the high-field conditions. The $\{g\}$ and $\{D_{Cr}\}$ tensors were subsequently transformed to the axes of $\{D_{12}\}$, using angles $\alpha$, $\beta$, and $\gamma$ found above. The 16 × 16 (complex) matrix of Hamiltonian (6) that included all $J$, $j$, $\{D_{Cr}\}$, $\{D_{12}\}$, and Zeeman terms was diagonalized by using the Householder transformation.[31] The resonance fields were found by an iterative procedure. When a resonance field was found, the eigenvectors of the Hamiltonian were evaluated and the expectation values of $\hat{S}^2$ for the levels $\psi_i$ and $\psi_j$ involved in a transition were computed. This was done to assign a transition to one of the $S = 1$, 2, or 3 states, which was necessary because the EPR line widths in different spin states are considerably different (Figures 5−9). The relative transition probability was evaluated from terms of the form

$$P = |\langle\psi_i|\mathbf{U}\{g_1\}\hat{\boldsymbol{S}}_1 + \mathbf{U}\{g_2\}\hat{\boldsymbol{S}}_2|\psi_j\rangle|^2 \qquad (16)$$

where **U** represents the unit-length vector perpendicular to the steady magnetic field ***B***. A total of 12 orientations of **U** were used, and the resulting $P$ values were averaged. The intensity of a transition was taken as a product of the probability $P$ and the population difference between the levels $\psi_i$ and $\psi_j$ obtained from the Boltzmann distribution. The above procedure was repeated thousands of times for various orientations of the steady magnetic field ***B*** to obtain a powder EPR spectrum.

The resulting simulations are shown in Figures 6, 8, and 9. Considering the complexity of the problem, they should be deemed as very good. The resonance line positions and relative intensities are very well reproduced in the wings of the spectra, which include resonances coming from all three spin states. Problems seen in the central part of the spectra may have a number of causes, like noncoaxiality of the $\{g\}$ and $\{D_{Cr}\}$ tensors and the line-width dependence on orientation, which was not taken into account. The simulations shown in Figures 6, 8, and 9 may represent the first successful application of the full Hamiltonian (6) to chromium(III) dimers. In papers published previously, mainly the X-band EPR was used with occasional application of both lower frequencies ($S$)[25] and moderately higher ($Q$),[22j,25] at which septet and triplet states could not be observed at all, or only partially,[23c,d,25] thus making the determination of $D_{Cr}$ problematic. Interestingly, in ref 25, it was estimated through its second-order effect on the low-frequency (S-band) $S = 2$ spectra. The zfs parameters for $S = 1-3$ determined from X-band spectra of ($\mu$-hydroxo)-bis[pentaamminechromium(III)] chloride monohydrate could not be reconciled with formulas (13),[23d] and it was concluded that Hamiltonian (6) is not suitable for solving the problem of chromium dimers. However, the zfs parameters for $S = 1$ as well as $D_{Cr}$ in ref 23d appear to be far too small in view of the present paper and most likely resulted from insufficient information available from the X-band EPR spectra. Also, the relative orientation of the $\{D_{12}\}$ and $\{D_{Cr}\}$ tensors was not considered. The conclusion from our work is that Hamiltonian (6) is fully adequate, but its application is difficult, owing mainly to noncoaxiality of the $\{D_{Cr}\}$ and $\{D_{12}\}$ tensors. Also, the problem could be solved, in principle, by using an X-band instrument equipped with a sufficiently strong magnet (see Figure 9) but finding the parameters would be even more difficult. The features in powder EPR spectra are observed at so-called turning points corresponding to the molecular orientations at which the resonance field passes through a maximum or minimum when a molecule is rotated versus the magnetic field. Such turning points in the high-field spectra occur only at the canonical orientations X, Y and Z, making assignment of the resonances easy, opposite to the X band, where many off-axial turning points are seen in a powder spectrum (Figure 9). Also, the $\Delta M_S = 1$ and 2 lines overlap in the X-band spectra but not in the high-frequency spectra.

**Estimation of $D_c$ and $E_c$ by DFT Calculations.** In order to determine experimentally the $D$ magnitude on an individual metal ion in a binuclear complex, doped dimers are sometimes prepared with one of the paramagnetic ions replaced by a diamagnetic metal ion, like $Ga^{3+}$ for $Fe^{3+}$.[29c] This is not possible in the present case, and therefore the magnitude of $D_{Cr}$ cannot be verified experimentally.

(31) Wilkinson, J. H. *The Algebraic Eigenvalue Problem*; Clarendon Press: London, 1970.

**Table 4.** Single-$Cr^{III}$ zfs Parameters Calculated from DFT

| experimental zfs parameters | functional and the SOC calculation method[a] | $D_{Cr}$, $cm^{-1}$ | $E_{Cr}$, $cm^{-1}$ |
|---|---|---|---|
| **1** | BP86, PK | 0.60 | 0.15 |
| $D_{Cr} = 0.386\ cm^{-1}$, | BP86, QRO | 0.42 | 0.14 |
| $E_{Cr} = 0.110\ cm^{-1}$ | BP86, CP | 0.66 | 0.18 |
| | B3LYP, QRO | 0.56 | 0.16 |
| **2** | BP86, PK | 0.91 | 0.20 |
| $D_{Cr} = 0.356\ cm^{-1}$, | BP86, QRO | 1.08 | 0.09 |
| $E_{Cr} = 0.065\ cm^{-1}$ | BP86, CP | 0.98 | 0.22 |
| | B3LYP, QRO | 1.14 | 0.12 |

[a] SOC = spin−orbit coupling, PK = Pedersen−Khanna, QRO = quasi-restricted orbitals, and CP = coupled−perturbed.[34]

We have thus attempted to calculate $D_{Cr}$ at the DFT level by using the software package *ORCA*.[32] In doing so, the full X-ray structure of the dimer was used in which one $Cr^{III}$ was replaced by $Ga^{III}$. The *ORCA* calculation utilized Ahlrichs-type basis set TZVPP[33a] for Cr and VDZP[33] for other atoms, combined with the BP86[33d,e,34] or BP3LYP[33d,e,35] functionals. Ahlrichs polarization functions from basis H-KrR and auxiliary bases from the *Turbomole* library were also used.[33c] For the spin−orbit-coupling (SOC) part of the zfs calculation, the Pederson−Khanna (PK), the "quasi-restricted orbitals" (QRO), and the coupled−perturbed (CP) methods[33,36] were tried (see Table 4). The spin−spin contribution to the zfs tensor was also evaluated.[36] The results were dependent on the method used, with the QRO giving $D_{Cr}$ closest to the magnitude found above for **1**, while calculations for **2** appear to be less successful, although in each case a correct sign of $D_{Cr}$ was obtained and the agreement was much better than 1 order of magnitude. Zein et al. found in a systematic study[36b] that the *D* values calculated from DFT are typically substantially overestimated, and no improvement results from employing basis sets larger than the standard SVP or TZVP or from using functionals other than BP.

Interestingly, the direction of the largest component of the calculated $\{D_{Cr}\}$ tensor forms a 97° angle with the Cr−Cr vector in **1** and a 123° angle in **2**, while angles of ca. 105° in both **1** and **2** result from the α, β, and γ angles found through the EPR simulation procedures above.

There are some reports of EPR studies on mononuclear chromium(III) complexes with mixed N,O coordination. Weyhermüller et al.[37] reported $D_{Cr} = 0.6\ cm^{-1}$ and $E_{Cr} = 0.12\ cm^{-1}$ in a methylamino-*N*,*N*-bis(2-methylene-4,6-dimethylphenol) complex with a $N_2O_4$ donor set. $D_{Cr} = 0.2\ cm^{-1}$ was observed in $N_3O_3$ coordination.[25] Complexes with only N donors exhibit *D* values over a similar range,[38] and, in general, *D* in $Cr^{III}$ rarely exceeds $0.4\ cm^{-1}$.[39]

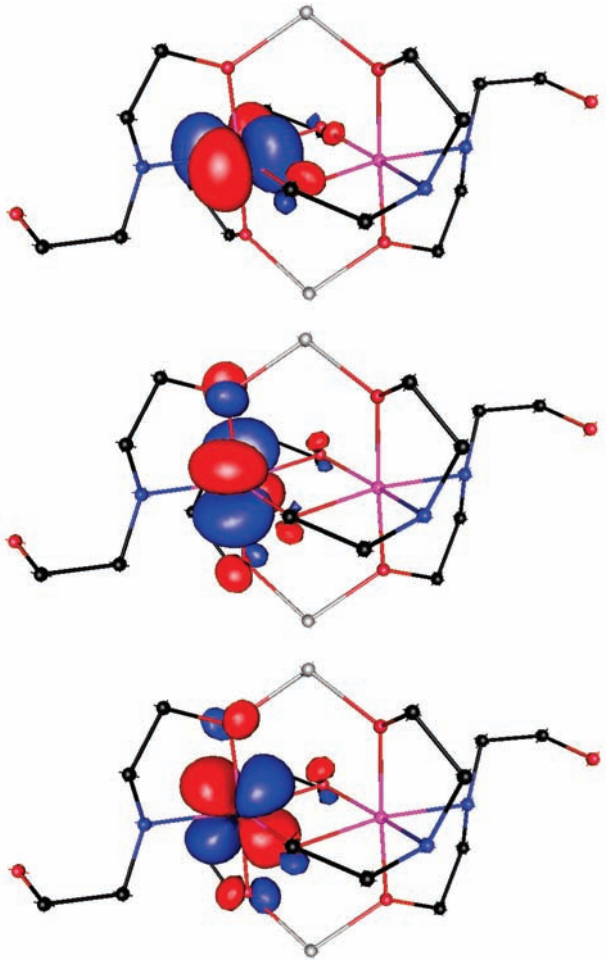

**Figure 10.** Magnetic orbitals of one of the $Cr^{III}$ ions in the "broken-symmetry"state. The dark-red, black, blue, magenta,and gray lines and spheres represent the O, C, N, Cr,and Zn atoms, respectively. The $SCN^-$ anions and H atoms were removed for clarity. "Spin-up" orbitals localized on one of the Cr atoms are shown. The corresponding "spin-down" orbitals have the same shape and are localized on the other Cr atom. The overlap integrals between corresponding "spin-up" and "spin-down" orbitals in **1** are 0.064, 0.048, and 0.005 for the top, center, and bottom plots, respectively, indicating the relative importance of these exchange pathways in the antiferromagnetic coupling. The analogous overlaps in **2** are 0.064, 0.052, and 0.013, respectively.

**Exchange Integrals in 1 and 2.** Calculation of the exchange integral *J* was attempted by applying the "broken-symmetry" approach available in the *ORCA* package. Full X-ray structures including $Zn(SCN)_2$ were used. In the broken-symmetry formalism, one places $N_A$ unpaired electrons localized on site A and $N_B$ unpaired electrons localized on a site B and performs two separate spin-unrestricted self-consistent-field calculations: the first one is for the high-spin state with a total spin equal to $(N_A + N_B)/2$ and the second is a "broken-symmetry" calculation with $N_A$ spin-up orbitals that are quasi-localized on site A and $N_B$ spin-down orbitals that are localized on site B (Figure 10).

(32) Neese, F. *ORCA—an ab initio, Density Functional and Semiempirical Program Package*, version 2.6-35; Universität Bonn: Bonn, Germany, 2008; free download from http://www.thch.uni-bonn.de/tc/orca/, registration required.

(33) (a) Schaefer, A.; Horn, H.; Ahlrichs, R. *J. Chem. Phys.* **1992**, *97*, 2571–2577. (b) Ahlrichs, R. et al., unpublished. (c) The Ahlrichs auxiliary basis sets were obtained from the *Turbomole* basis set library under ftp.chemie.uni-karlsruhe.de/pub/jbasen. (d) Eichkorn, K.; Treutler, O.; Ohm, H.; Haser, M.; Ahlrichs, R. *Chem. Phys. Lett.* **1995**, *240*, 283–289. (e) Eichkorn, K.; Weigend, F.; Treutler, O.; Ahlrichs, R. *Theor. Chem. Acc.* **1997**, *97*, 119–124.

(34) (a) Becke, D. A. *Phys. Rev. A* **1988**, *38*, 3098–3100. (b) Perdew, J. P. *Phys. Rev. B* **1986**, *33*, 8822–8824. (c) Perdew, J. P. *Phys. Rev. B* **1986**, *34*, 7406–7406. (c) Kendall, R. A.; Früchtl, H. A. *Theor. Chem. Acc.* **1997**, *97*, 158–163.

(35) (a) Lee, C.; Yang, W.; Parr, R. G. *Phys. Rev. B* **1988**, *37*, 785–789. (b) Becke, A. D. *J. Chem. Phys.* **1993**, *98*, 5648–5652. (c) Stephens, P. J.; Devlin, F. J.; Chabalowski, C. F.; Frisch, M. J. *J. Phys. Chem.* **1994**, *98*, 11623–11627.

(36) (a) Neese, F. *J. Am. Chem. Soc.* **2006**, *128*, 10213–10222. (b) Zein, S.; Duboc, C.; Lubitz, W.; Neese, F. *Inorg. Chem.* **2008**, *47*, 134–142.

(37) Weyhermüller, T.; Paine, T. K.; Bothe, E.; Bill, E.; Chaudhuri, P. *Inorg. Chim. Acta* **2003**, *337*, 344–356.

(38) Pedersen, E.; Toftlund, H. *Inorg. Chem.* **1974**, *7*, 1603–1612.

(39) Krzystek, J.; Ozarowski, A.; Telser, J. *Coord. Chem. Rev.* **2006**, *250*, 2308–2324.

The TZVPP basis set was used for Cr atoms, and SVP functions were used for all other atoms. (A dramatic failure resulted from using SVP functions for Cr, while using TZVPP functions for atoms other than Cr did not affect the results.) Replacing the two dangling $CH_2OH$ groups by H atoms to reduce the number of atoms in calculations had no effect on $J$. The exchange integrals were calculated according to the convention $J = 2(E_{HS} - E_{BS})/(\langle S_{HS}^2\rangle - \langle S_{BS}^2\rangle)$, where HS and BS denote the high-spin and broken-symmetry states, respectively.[40] The original formula for $J$ from *ORCA*, which uses the exchange Hamiltonian $\hat{H} = -2J\hat{S}_a\hat{S}_b$, was converted to the notation of this paper by multiplying it by −2. Functional B3LYP was used, which was reported to give the best results in the "broken-symmetry" method.[41] $J$ values of 9.0 and 11.6 $cm^{-1}$ were found for 1 and 2, respectively, in reasonable agreement with the experiment. It is very difficult to pinpoint structural differences between 1 and 2 that could be responsible for the difference in the exchange coupling because the structures are very similar. The Cr−O−Cr angle in 2 is only very slightly smaller than that in 1 (99.0° vs 99.3°). A complicating factor is that the Me−O−Zn−O−Me bridges are also known to transmit exchange interactions. Relatively strong antiferromagnetic exchange mediated by two Cu−O−Zn−O−Cu bridges, with $J = 35$ $cm^{-1}$, was observed in the heterometallic diethanolamine complex $[Cu_2Zn_2(NH_3)_2Br_2(HDea)_4]Br_2\cdot CH_3OH$.[42a] Weak ferromagnetic interactions between two $Cu^{2+}$ ions[42b] and weak antiferromagnetic interactions between two $Cr^{3+}$ ions[25] mediated by a $Zn(dmg)_3$ bridge (dmg = dimethylglyoximate) were reported. In the present system, the in-plane Cr−O−Cr interactions are mainly responsible for the magnetic properties. The magnetic orbitals of the Cr ions (see Figure 10), which involve the in-plane O3 atoms (Figure 1), involve also the out-of-plane O1 and O4 atoms, which are bound to Zn. Calculations with the two $Zn(SCN)_2$ groups removed yield moderately increased $J$ magnitudes (13.0 $cm^{-1}$ for 1 and 15.2 $cm^{-1}$ for 2). Removal of the $Zn(SCN)_2$ groups from calculations resulted in an increase in the electron and spin densities on the bridging O atoms, while the electronic density on the out-of-plane O atoms decreased. Also, the three overlap integrals between the magnetic orbitals shown in Figure 10 changed to 0.071, 0.042, and 0.007, respectively. This may indicate that the presence of the Zn ions inhibits the in-plane Cr−O−Cr exchange pathways rather than providing additional ferromagnetic pathways Cr−O−Zn−O−Cr.

Finally, it should be mentioned here that DFT calculations of $J$ for simple model systems have also been reported.[43]

**Exchange Contribution to the zfs Parameters in Chromium(III) Dimers.** The $\{D_{12}\}$ tensor consists of dipole−dipole and anisotropic exchange interactions. Formulas (15) with $R_{Cr-Cr} = 3.01$ Å and $g_x = g_y = g_z = 1.983$ yield $D_{xx}^{dipolar} = 0.0624$ $cm^{-1}$, $D_{yy}^{dipolar} = 0.0624$ $cm^{-1}$, and $D_{zz}^{dipolar} = -0.1248$ $cm^{-1}$, while the $\{D_{12}\}$ components are 0.0469, 0.0779, and −0.1248 $cm^{-1}$ in **1** and 0.0505, 0.0729, and −0.1233 $cm^{-1}$ in **2**. The *zz* component of the $\{D_{12}\}$ tensor thus appears to be fully determined by the dipole−dipole interactions. However, the difference between the *xx* and *yy* components cannot be interpreted within the dipolar model. In the simplest point−dipole implementation (eq 15) the $D_{xx}$ and $D_{yy}$ components must be equal and the dipolar contribution to $E_{12}$ must equal 0. We have tried to use a model in which a dipole on each Cr atom is split into 12 parts located along the lobes of the $d_{xy}$, $d_{xz}$, and $d_{yz}$ orbitals at a 0.5 Å distance from the respective Cr atoms. The dipolar tensor components can then be calculated by adapting formula (3) in ref 28 to the present case:

$$D_{\alpha\gamma} = \mu_B^2 g_\alpha g_\gamma \sum_{i=1}^{12}\sum_{j=1}^{12}(\delta_{ij} - 3\sigma_i\sigma_j)/144R^3 \qquad (17)$$

where $g_\alpha$ and $g_\beta$ are the $g$ components, $R$ is the Cr−Cr distance, $\delta_{ij}$ is Kronecker's delta, and $\sigma_i$ and $\sigma_j$ are the cosines of the angles between the vector **R** and a vector joining the partial dipoles $i$ and $j$. This approach slightly changed $D_{zz}^{dipolar}$ from −0.1248 to −0.1272 $cm^{-1}$ but, despite the slight asymmetry of the $Cr_2O_6N_4$ core, generated the dipolar contribution to $E_{12}$ of only about $^1/_{60}$ of the observed magnitude. Therefore, a small anisotropic exchange contribution cannot be excluded. Taking **1** as an example, we subtract the $\{D^{dipolar}\}$ components from the $\{D_{12}\}$ components to obtain the "excess" values −0.0155, +0.0155, and 0 $cm^{-1}$, which are possibly associated with the anisotropic exchange. The components of the anisotropic exchange tensor are expected to be on the order of magnitude of $(g - g_e)^2 J_{exc}$, where the free-electron $g_e$ value equals 2.0023 and $J_{exc}$ is the exchange integral in an excited state of a dimer, in which one of the $Cr^{3+}$ ions is in its electronic ground state while the other one is in its excited state.[27a,30b,c,44] In our case, the latter expression yields $4 \times 10^{-4} J_{exc}$, and to get the anisotropic exchange components like 0.0155 $cm^{-1}$, $J_{exc}$ would have to be about 40 $cm^{-1}$, which is not unthinkable. In copper(II) dimers, $J_{exc}$ of much larger magnitude than $J$ is typically found from similar procedures.[27a,45] Extracting $J_{exc}$ from experiments other than EPR is extremely difficult and, to our knowledge, has been attempted only for copper(II) dimers[46] (see also ref 27a).

Some literature data also suggest that the anisotropic exchange may contribute to the zfs parameters in chromium dimers. Glerup and Weihe[23d] have determined the $D_{12}$ and $E_{12}$ parameters in the quintet state of a $\mu$-OH-bridged complex $[(NH_3)_5CrOHCr(NH_3)_5]Cl_5\cdot H_2O$ from X-band EPR spectra. After conversion to the notation used in this paper, their parameters result in $D_{12} = -0.15$ $cm^{-1}$

(40) (a) Yamaguchi, K.; Takahara, Y.; Fueno, T. In *Applied Quantum Chemistry*, Smith, V. H., Ed.; Reidel: Dordrecht, The Netherlands, 1986; p 155. (b) Soda, T. et al. *Chem. Phys. Lett.* **2000**, *319*, 223.

(41) (a) Rodriguez-Fortea, A.; Alemany, P.; Alvarez, S.; Ruiz, E. *Chem.—Eur. J.* **2001**, *7*, 627–637. (b) Ruiz, E.; Alvarez, S.; Cano, J.; Polo, V. *J. Chem. Phys.* **2005**, *123*, 164110. (c) Ruiz, E.; Alemany, P.; Alvarez, S.; Cano, J. *J. Am. Chem. Soc.* **1997**, *119*, 1297–1303.

(42) (a) Buvaylo, E. A.; Vladimir, N.; Kokozay, V. N.; Vassilyeva, O. Yu.; Skelton, B. W.; Jezierska, J.; Brunel, L. C.; Ozarowski, A. *Chem. Commun.* **2005**, 4976–4978. (b) Ruiz, R.; Julve, M.; Faus, J.; Lloret, F.; Muñoz, M. C.; Journaux, Y.; Bois., C. *Inorg. Chem.* **1997**, *36*, 3434.

(43) Bencini, A.; Totti, F. *Inorg. Chim. Acta* **2008**, *361*, 4153–4156.

(44) (a) Bleaney, B.; Bowers, K. D. *Proc. R. Soc. London, A* **1952**, *214*, 451–465. (b) Gribnau, M. C. M.; Keijzers, C. P. *Inorg. Chem.* **1987**, *26*, 3413–3414.

(45) (a) Ozarowski, A.; Reinen, D. *Inorg. Chem.* **1986**, *25*, 1704–1708. (b) Kahn, O.; Galy, J.; Journaux, Y.; Morgenstern-Badarau, I. *J. Am. Chem. Soc.* **1982**, *104*, 2165–2176. (c) Boilot, M. L.; Journaux, Y.; Bencini, A.; Gatteschi, D.; Kahn, O. *Inorg. Chem.* **1985**, *24*, 263–267.

(46) Ross, P. K.; Allendorf, M. D.; Solomon, E. I. *J. Am. Chem. Soc.* **1989**, *111*, 4009–4021.

and $E_{12} = -0.026\ cm^{-1}$, while the dipole−dipole contributions (converted from data in ref 23d) are $-0.09\ cm^{-1}$ and 0, respectively. In a dimeric dihydroxo-bridged chromium(III) complex of 1,4,8,11-tetraazacyclotetradecane (cyclam),[23c] $D_{12}$ (and, consequently, $D_{S=2}$) appears to be largely consistent with the dipolar interactions only, but a large $E_{12}$ parameter again indicates a contribution due to the anisotropic exchange, which was indeed postulated.

## Conclusions

The compounds reported here are quite rare examples of chromium complexes with an amino alcohol. It was shown that, under the direct synthesis conditions, Reinecke's salt acts as a source of Cr ions but not as a metalloligand nor as a building block. Variable-temperature magnetic susceptibility shows weak intramolecular antiferromagnetic coupling between Cr ions. High-field, high-frequency EPR spectra allowed a reliable determination of the single-ion contribution to the zfs parameters in each complex. It is shown that EPR spectra of chromium(III) dimers can be simulated by using Hamiltonian (6) provided that the relative orientation of the $\{D_{Cr}\}$ tensor versus the $\{D_{12}\}$ tensor is taken into account. The magnitudes of the zfs parameters on separate Cr ions as well as of the isotropic exchange interactions were estimated by DFT calculations. Anisotropic exchange interactions appear to contribute little to the zfs.

**Acknowledgment.** This work was supported by the Victor Pinchuk Foundation, by the Fundamental Researches Fund of Ukraine (Project 28.3/017), APVV Slovakia (Project VVCE-0004-07), and by NHMFL, which is funded by the NSF through Cooperative Agreement No. DMR-0654118, the State of Florida, and the DOE.

**Supporting Information Available:** CIF file for **1** and **2**, effect of the biquadratic exchange on magnetic susceptibility (Figure S1), energy levels of **2** in a magnetic field (Figure S2), effect of spin-state mixing on EPR spectra (Figure S3), zfs effect on the magnetic susceptibility (Figure S4), table of molar magnetic susceptibilities for **1** and **2** (Table S1), and shortened output of the "broken-symmetry" calculation for **1**. This material is available free of charge via the Internet at http://pubs.acs.org. Crystallographic data for compounds **1** and **2** have also been deposited with the Cambridge Crystallographic Data Centre and are available at www.ccdc.cam.ac.uk/data_request/cif under deposition numbers CCDC 747969−747970.